Published in final edited form as:
FEBS Lett. 2009 January 22; 583(2): 456–464. doi:10.1016/j.febslet.2008.12.046.

Characterization of the *C. elegans Islet* LIM-homeodomain ortholog, *lim-7*

Roumen Voutev[1,2], **Ryan Keating**[3], **E. Jane Albert Hubbard**[1,4], and **Laura G. Vallier**[3,§]

[1] Developmental Genetics Program, Skirball Institute of Biomolecular Medicine, New York University School of Medicine, New York, NY 10016

[2] Department of Biology, New York University, New York, NY 10003

[3] Department of Biology, Hofstra University, Hempstead, NY 11549

[4] Department of Pathology and Helen and Martin Kimmel Center for Stem Cell Biology, New York University School of Medicine, New York, NY 10016

Abstract

lim-7 is one of seven *C. elegans* LIM-homeodomain (LIM-HD)-encoding genes and the sole *Islet* ortholog. LIM-HD transcription factors, including *Islets*, function in neuronal and non-neuronal development across diverse phyla. Our results show that a *lim-7* deletion allele causes early larval lethality with terminal phenotypes including uncoordination, detached pharynx, constipation and morphological defects. A *lim-7*(+) transgene rescues lethality but not adult sterility. A *lim-7*(+) reporter in the full genomic context is expressed in all gonadal sheath cells, URA neurons, and additional cells in the pharyngeal region. Finally, we identify a 45-bp regulatory element in the first intron that is necessary and sufficient for *lim-7* gonadal sheath expression.

Keywords

LIM-homeodomain; transcription factor; *C. elegans*; gonadal sheath; pharynx; Pun

1. Introduction

LIM-Homeodomain (LIM-HD) transcription factors comprise a widely conserved family whose members are characterized by two LIM domains, each of which consists of two specialized zinc fingers, that are located amino-terminally to a DNA-binding homeodomain [1]. LIM-HD proteins are well studied in the context of motorneuron patterning in diverse phyla [2]. LIM-HD family members also have roles, together with other transcription factors, in a variety of non-neuronal tissues such as in myocardial progenitors in mouse, zebrafish, and *Drosophila* [3–6] and in vulval and uterine morphogenesis in *C. elegans* [7].

There are seven *C. elegans* LIM-HD proteins with at least one falling into each of the six subclasses of the LIM-HD family based on conserved features within the homeodomain [1]. All the *C. elegans* LIM-HD proteins are expressed neuronally [1] and four are additionally

§To whom correspondence should be addressed.

expressed non-neuronally. The Islet protein, one of the LIM-HD family founding members (the "I" in the LIM acronym), was originally isolated through its ability to bind upstream sequences of the rat insulin gene [8]. The Islet subclass contains transcription factors that function in motorneuron development, pathfinding and identity as well as in the development of non-neural tissues [1,9,10]. The *C. elegans* LIM-7 transcription factor is the only LIM-HD Islet subclass member [1]. Previous work demonstrated that a *lim-7::GFP* reporter expresses in four URA motorneurons in the head and in a subset of the non-neuronally derived gonadal sheath cells, [11,12]. Therefore, *C. elegans* is a favorable system to explore the function of Islet transcription factors using *lim-7*, the sole Islet ortholog.

In this study, we present genetic analysis of *lim-7*, based on a 1345-bp deletion allele, and expression pattern studies. We show that loss of *lim-7* results in early larval lethality associated with pleiotropic L1 larval defects and that *lim-7*(+) rescues this lethality. Our expression analysis extends the previously reported expression pattern. Finally, we demonstrate that the large first intron of *lim-7* contains regulatory sequences necessary and sufficient for gonadal sheath expression.

2. Materials and Methods

2.1 Nematode Strains

C. elegans strains were cultured using standard genetic procedures [13] at 20°C. The following available strains were used: N2 (Bristol) wild type [13]; DG1575 (*tnIs6*[*lim-7::GFP; rol-6 (su1006)*] V) [11].

HN9 and HN29 carry the *lim-7*(*tm674*) allele and both are of the genotype *lim-7*(*tm674)/hT2* [*bli-4(e937) let-?*(*q782*) *qIs48*[(*myo-2::GFP pes-10::GFP ges-1::GFP*)]] (I;III). We used the *hT2*[*bli-4*(*e937*) *let-?*(*q782*) *qIs48*] (I;III) balancer, designated hereafter as "*hT2*[*let GFP*]". HN9 and HN29 result from five and seven outcrosses, respectively. Each outcross was done by first crossing *tm674/hT2* to N2 and then crossing *tm674/+* progeny back into the balancer. Non-balanced chromosomes underwent twice the number of outcrosses. Outcrossed strains were assayed by PCR to ensure the presence of *tm674*. All outcrossed strains examined had identical phenotypes.

HN15 is one of three strains that carries the *lim-7*(+) WRM061aF09 fosmid on an extrachromosomal array in the *lim-7*(*tm674*) background. (See below section 2.2 for information on the generation of the arrays). Two other similar lines were crossed into the *lim-7* (*tm674*) background and while all behaved identically, the bulk of the analysis was performed on HN15. HN15 was constructed by crossing *+/hT2*[*let GFP*] males to HN13 (*lvEx4*[*lim-7*(+), *sur-5::GFP*]) hermaphrodites (see below) and selecting *hT2*[*let GFP*]/+; *lvEx4* males to cross to HN9. Resulting progeny with a GFP(+) pharynx and GFP(+) body nuclei (genotype *hT2* [*let GFP*]/*tm674; lvEx4*) were selected for analysis.

RW10289 ((*stIs10289*[*lim-7*(+)*::GL-mCherry-3xFLAG, unc-119*(+)]*; unc-119*(*e2498*)), in which *stIs10289* contains the same fosmid, WRM061aF09, as in *lvEx4* except that it was recombineered to have the *lim-7* genomic region fused to a carboxyl-terminal mCherry tag [14] and a 3xFLAG epitope in *stIs10289* (non-native sequences optimized for worm codon bias). Only *lim-7* and the downstream gene C04F1.1 are contained on the fosmid in their entirety.

GC889 (*naIs8*[pGC361 (*lim-7*(*intron1::mCherry*), (*Cb*)*unc-119*(+))] V; *ceh-18*(*1082*) X) was made by crossing RB1103 (*ceh-18*(*ok1082*) X) to *naIs8*[*lim-7*(*intron1::mCherry*, (*Cb*)*unc-119* (+)]/+ V males and screening for homozygous *ceh-18*(*ok1082*) and *lim-7*(*intron1::mCherry*)

cross progeny. The *naIs8* allele arose from microparticle bombardment of pGC361 (see below) into *unc-119*(*ed3*) worms.

GC1008 (*naIs8*[*lim-7*(*intron1::mCherry*), (*Cb*)*unc-119*(+)] V; *ceh-18*(*mg57*) X) was constructed as for GC889 substituting *ceh-18*(*mg-57*).

2.2 Generation and analysis of transgenic strains and RNAi reagents

A transgenic line carrying *lvEx4*[*lim-7*(+), *sur-5::GFP*] was generated by co-injection of WRM061aF09 at 1 ng/μl, pTG96 (containing *sur-5::GFP*) at 50 ng/μl and pBluscript SK+ at 100 ng/μl into N2 worms. Four transmitting lines, including *lvEx4*, were selected; one representative line is HN13. Five transgenic lines carrying fosmid WRM065cH02 were generated by co-injection of WRM065cH02 at 1 ng/μl, pTG96 (containing *sur-5::GFP*) at 10 ng/μl and pRF4[*rol-6(su1006)*] at 100 ng/μl into *dpy-5(e61) unc-13(e51)*/*lim-7(tm674)*. Three transgenic lines carrying fosmid WRM0614aG01 were generated by co-injection of WRM0614aG01 at 1 ng/μl and pRF4 at 100 ng/μl into *dpy-5(e61) unc-13(e51)*/*lim-7 (tm674)*. To generate these same transgenic lines in *hT2*[*let GFP*]/*lim-7*(*tm674*) background, all WRM065cH02 and WRM0614aG01 transgenic lines were crossed into the *hT2*[*let GFP*] background by mating to *hT2*[*let GFP*]/*unc-119(ed3)* males and selecting roller hermaphrodites expressing *hT2*[*let GFP*] not segregating Dpy Unc animals (genotype *lim-7 (tm674)/hT2*[*let GFP*] [*fosmid array*]).

To generate strains carrying plasmids pGC197, pGC226, pGC348, pGC357, pGC421, and a linearized fragment from pGC433 or PCR products PCR[707-814], PCR[690-735] and PCR [690-719] (Figure 1A, see also below), N2 worms were injected with the respective plasmid, linearized DNA or PCR product at a 10 ng/μl concentration together with pRF4 [15] at 100 ng/μl.

We note that we sequenced the mv_C04F1.3 cDNA (Open Biosystem ORFeome clone RCE 1182-9363645) and found that it carries *lim-7*, however this cDNA does not include exon 6. This cDNA (which splices exon 5 to exon 7) introduces numerous premature stop codons, which would preclude translation of the homeodomain. It is unlikely that this cDNA encodes a functional LIM-domain-only isoform of *lim-7*. To confirm *lim-7* gene structure, we amplified a full-length *lim-7* cDNA from the ProQuest™ *C. elegans* cDNA library using primer pairs CTTCTATATCTGTTCAACGGC and AACTATTCTCCACACGGCGC and inserted the product in pCR-XL-TOPO (Invitrogen), resulting in pGC471. We sequence-verified the cDNA we obtained and found that it is consistent with the predicted *lim-7* gene structure and previously isolated mRNA for the gene (EMBL mRNA accession number U73946; O. Hobert and G. Ruvkun, personal communication).

2.3 Detection of locus deletions

Standard methods were used to manipulate plasmid DNA and oligonucleotides. To detect the *tm674* deletion, 5′-TGCTCAAGACAAGAGACGGA-3′ and 5′-GAAGGCTTCGCAAAAAGATG-3′ oligonucleotides were used to amplify the relevant *lim-7* region using the Expand Long Template PCR System (Roche Applied Science).

The *ceh-18*(*ok1082*) allele is a 2143-bp deletion, verified by PCR amplification using primers 5′CGATGTTGCGTTCATAGTGG-3′ and 5′-CGCCCAAAATTTTTCATCAT-3′, followed by sequencing; *ok1082* removes parts of intron 3 and exon 3, including the splice donor in intron 3. The sequence flanking the deletion is: 5′-TGGCATCGCTCAGGCAAATAGCGAA-3′ and 5′-GTCGATGAATTGGTGTGCGCCCAAC-3′.

2.4 Microscopy

Worms were visualized using a Zeiss AxioImager equipped for DIC and fluorescence microscopy, and images were captured using an Axiocam camera and AxioVision software. Determination of the stage of lethality was performed on an Olympus SZX epifluorescent dissecting microscope equipped with a GFP filter.

2.5 Phenotypic analysis of *lim-7 (tm674)*

For determination of stage of lethality, a modified hatch-off was used to synchronize larvae [16]. Briefly, HN9 (*tm674/hT2*[*let GFP*]) hermaphrodites laid eggs overnight at 20°C on NGM plates [13]. Larvae and adults were washed off with M9 [17]. Remaining embryos hatched at 20°C for two-hour cycles (3–4 cycles per experiment; ≥3 experiments). Only five-sixteenths of embryos segregating from *hT2*[*let GFP*] heterozygotes are potentially viable [18,19]. GFP-expressing and non-expressing larvae were tallied as percentage of total larvae (Table 1).

For determination of pharyngeal detachment, a hatch-off from HN29 (*tm674*/*hT2*[*let GFP*]) mothers was performed essentially as above, collecting synchronized L1 larvae after two hours and examining them either immediately or 8–10 hours later. Pharyngeal attachment/detachment was scored at each time point. The experiment was repeated 2–3 times; combined data are presented as percentage of total.

For the analysis of the L1 *lim-7*(*tm674*) phenotype, L1 larvae that did not express GFP (*tm674* homozygotes) were either directly examined from mixed-stage cultures or from synchronized embryos. Newly hatched L1 larvae were washed with M9 and briefly centrifuged at ~1200 rpm. Larvae were collected with a Pasteur pipette and distributed to 60 mm NGM plates seeded with OP50 *E. coli*. GFP(−) L1 larvae (*tm674* homozygotes) were examined using DIC optics at 400–1000X magnification and penetrance of mutant phenotype tallied as a percentage of total *tm674* larvae.

2.6 Enhancer identification

The original $P_{lim\text{-}7}$*::GFP* reporter construct in *tnIs6* is a 4.13 kb *Pst*I-*Bam*HI genomic fragment from *lim-7*. This fragment includes 2.23 kb of the upstream region, the entire first exon, the first intron, and part of the second exon translationally fused to GFP in pPD95.75 [11]. To generate pGC197 (see Figure 1A), a *Sca*I-*Bam*HI fragment (first intron with part of the second exon fused to GFP) was isolated from the original $P_{lim\text{-}7}$*::GFP* reporter construct and was ligated to *Hin*cII/*Bam*HI-cut pPD95.75 (http://www.addgene.org/1494). The remaining plasmids depicted in Figure 1A were constructed as follows. *Psi*I-*Bam*HI, *Bgl*II-*Sma*I, and *Bsa*I-(blunted)-*Xma*I fragments were sequentially cut from pGC197 and subcloned into *Hin*cII/*Bam*HI-, *Bam*HI-*Sma*I-, and *Hin*cII/*Xma*I-digested pPD95.75 to create pGC226, pGC346, and pGC357, respectively. Subsequently, to test whether the *Bsa*I-*Bgl*II *lim-7* intronic fragment drove GFP expression, the *Sph*I-*Bgl*II fragment from pGC357 was inserted into *Sph*I-*Bam*HI-digested pPD95.75 to create pGC421 (pPD95.75 appears to have a cryptic basal promoter [20]). The fragment was further refined by isolating a *Dra*I-*Bgl*II fragment from pGC357 and inserting it into *Hin*cII/*Bam*HI-cut pPD95.57, creating pGC433. The *Sph*I-*Spe*I-linearized pGC433 fragment [*lim-7(Dra*I-*Bgl*II *fragment)-GFP-unc-54(3′UTR)*] was used for injections [21]. PCR fragment PCR[707-814] was amplified from pGC433 using primer pairs GCTATTTCTTTCATTCCATTTGTCCCCCTC and CTAGTAGGAAACAGTTATGTTTGG. PCR fragment PCR[690-719] was amplified from pPD95.75 using primer pairs AAAAGAAAACAAAAATCGCTATTTCTTTCcccgggattggccaaaggacc (lower case letters indicate vector sequences) and CTAGTAGGAAACAGTTATGTTTGG. PCR fragment PCR [690-735] was amplified from pPD95.75 using primer pairs aagcatgcAAAAGAAAACAAAAATCGCTATTTCTTTCATTCCATTTGTCCCCCgggattg

gcca aaggaccc (lower case letters indicate vector sequences) and CTAGTAGGAAACAGTTATGTTTGG. pGC361 is a derivative of pGC197 with GFP replaced by mCherry and *C. briggsae unc-119* (+) added to the vector between *Spe*I and *Apa*I.

2.7 Bioinformatics

Sequences of intron 1 for *C. brenneri* and *C. remanei* were obtained by BLAST search (http://genome.wustl.edu/). The *C. elegans lim-7* cDNA query sequence identified the corresponding orthologous *lim-7* sequences for *C. brenneri* (in contig1054.3) and *C. remanei* (in contig228.2). Sequence comparisons of intron 1 among the four related species were performed in a pairwise manner (*C. elegans* intron 1 as query) using the NCBI BLAST alignment tool, bl2seq (http://www.ncbi.nlm.nih.gov/blast/bl2seq/wblast2.cgi) [22].

3. Results

3.1 *lim-7* (*tm674*) mutants die in the first larval (L1) stage

The *lim-7* gene encodes a 452-amino acid Islet-type LIM-HD transcription factor. Although a *lim-7* reporter has been used in the field for nearly a decade [11], there has been no functional analysis of this gene. We performed RNAi feeding using *lim-7* cDNA (see Materials and Methods 2.2) on homozygous wild-type and heterozygous (*tm674/hT2*[*let GFP*]) animals and found no discernable phenotype (data not shown). The failure to observe an RNAi phenotype for *lim-7* could indicate that the "knock-down" phenotype for the locus is "wild-type" or it could indicate that this gene is refractory to RNAi. Therefore, we investigated a 1345-bp deletion within *lim-7*(*tm674*), generated by the National Bioresource Project, that starts in intron 3 and ends in intron 5 (Figure 1). If a stable mutant protein were made by splicing exon 2 to exon 6, it would lack amino acids (aa) 84 to 161, which includes most of the first (aa 56-115) and second (aa 118-178) LIM domains, (based on Pfam predictions; Figure 1). Therefore, it is unlikely that this mutant protein would be functional. One prediction is that such a mutant protein might confer a dominant negative phenotype: the mutant protein homeodomain (aa 266-322) would still be able to bind DNA and could compete with wild-type protein for binding sites, and thereby reduce the ability of wild-type protein to form functional transcriptional activation complexes. However, our results indicate that the *tm674* mutation was recessive to wild type, consistent with *tm674* behaving as a simple loss-of-function allele.

To determine the *lim-7*(*tm674*) mutant phenotype, we examined *tm674* homozygotes segregating from HN9 (*tm674/hT2*[*let GFP*]) hermaphrodites. No adult or late-larval homozygous *tm674* progeny segregated from this strain, suggesting that *tm674* caused embryonic or early larval lethality. To test this hypothesis, embryos from HN9 hermaphrodites were synchronized and assessed at two-hour intervals post-hatching for the presence of *tm674* L1 larvae (see Materials and Methods 2.5). If lethality occurred during embryogenesis, all L1 larvae should express GFP (all living larvae would be heterozygous for the *hT2*[*let GFP*] balancer chromosome) but if lethality occurred during the L1 stage, one-fifth of the L1 larvae present should not express GFP because they would be *tm674* homozygotes. We found that 18% L1 larvae did not express GFP (Table 1), and all larvae surviving to the L2 larval stage expressed GFP. Therefore, *lim-7*(*tm674*) mutants die during the L1 larval stage.

3.2 Terminal pleiotropic defects of *tm674* L1 larvae

To examine the cause of lethality in *tm674* homozygotes, mutant larvae were examined for morphological defects. The most apparent phenotype was uncoordinated movement (Unc): most L1 larvae were unable to move or moved poorly. Reflecting this, 74% of the L1 larvae scored in still images had an abnormal body position (Table 2 and Figures 2 B and C), with

extra body bends or doubling over. The second most penetrant phenotype (43%) was an unattached pharynx (Pun; Table 2, Figure 2 A). Other phenotypes included intestinal constipation, dumpy (Dpy) body morphology (increased width to length ratio; compare Figures 2 A and C), body cavity vacuolization, and misshapen head morphology (Figure 2). Therefore, *lim-7*(*tm674*) confers 100% L1 lethality with a high degree of pleiotropy.

The Pun phenotype occurred during the L1 stage, as the pharynx was attached in all homozygous embryos observed (data not shown, n >100). In L1 larvae, the pharynx detaches from the labia near the arcade cells, which connect the labia to the pharynx. If L1 larvae hatch with an attached pharynx and it becomes detached over time, then a greater number of younger L1 larvae should retain an attached pharynx relative to older L1 larvae. To test this hypothesis, embryos were synchronized and *tm674* larvae were scored at early and late L1 time points (see Materials and Methods 2.5). At two hours, 66% (n=56) of *tm674* L1 larvae had an attached pharynx compared to 61% (n=31) at 10–12 hours. Thus, detachment does not appear to occur over time during the L1, suggesting that the labia-pharynx connection is fragile in these mutants.

The cause of the L1 lethality is still unresolved. In addition to the observed phenotypes that contribute to lethality, additional factors must contribute to lethality because 5% (n= 137) of L1 larvae exhibited no obvious defects.

3.3 *lim-7*(+) partially rescues *tm674*

To determine which *tm674* phenotypes were rescued by transgenic *lim-7*(+), we generated and examined three independent transgenic lines carrying fosmid WRM061aF09 on an extrachromosomal array in a *tm674* background (*tm674/hT2*[*let GFP*]; *lvEx*[*lim-7*(+), *sur-5::GFP*]), all of which behaved similarly. Transgenic animals of the genotype *tm674; lvEx4*[*lim-7*(+), *sur-5::GFP*] survived to adulthood. However, adult hermaphrodites were sterile. Gonads of rescued homozygous *tm674* adult hermaphrodites displayed several defects: reduced overall size, reduced number of germ cells and mature oocytes, ovulation defects and early embryo defects (Figure 4). These phenotypes are consistent with a defective gonadal sheath: robust germ line proliferation requires the distal sheath and ovulation requires the proximal sheath [12,23]. In addition, the presence of loose sperm suggested spermathecal rupture (Figure 4).

Three genes reside in their entirety on fosmid WRM061aF09, which is included in the partially rescuing transgenic arrays: the snoRNA T19B4.8, *lim-7*, and C04F1.1. To assure that the rescue seen is due to the presence of the transgenic *lim-7(+)* and not to the presence of the one of the other genes on WRM061aF09, additional transgenic lines that contain one of two different fosmids on simple extrachromosomal arrays were established in *tm674/hT2* [*let GFP*] hermaphrodites and assessed for rescue. The first fosmid, WRM065cH02 eliminates C04F1.1 and the second fosmid, WRM0614aG01 eliminates the snoRNA T19B4.8; both contain *lim-7* in its entirety. Five lines of WRM065cH02 were established and four of them rescued the lethality; adult hermaphrodites in those four lines were sterile or produced only 1–2 larvae, which died during the L1 larval stage. Three lines of WRM0614aG01 were established and two of the three showed the identical rescue as seen for both WRM061aF09 and WRM065cH02. Thus, neither C04F1.1 nor the snoRNA T19B4.8 is responsible for the rescue. Therefore, taken together these data indicate that transgenic expression of *lim-7*(+) rescued the larval lethality but revealed a possible additional requirement of *lim-7* for fertility (see Discussion).

3.4 The *lim-7*(+)*::mCherry* transgene extends the expression pattern beyond previously characterized transgenes

Given that earlier *lim-7* reporter constructs were not generated in a full genomic context, we compared previously characterized reporter expression to *lim-7*(+)*::mCherry* transgene expression in its genomic context (strain RW10289 (*stIs10289*); see Materials and Methods 2.1). The earlier reporters (*tnIs5* or *tnIs6*) express GFP in the four distal pairs of sheath cells (Sh1-4) surrounding each hermaphrodite gonad arm, in the four URA motorneurons in the head [11], and numerous tail neurons in the male (data not shown). Recently, using a smaller *lim-7* promoter sequence (1.5 kb) fused to GFP, Reece-Hoyt et al (2007) reported expression of *lim-7* at all stages of embryogenesis as well as in several tissues during larval and adult stages but not in the gonadal sheath [24]. In contrast, the *stIs10289* reporter used in this study contains the entire upstream and downstream genomic sequences plus the entire gene fused to mCherry and it displayed mCherry in all five pairs of gonadal sheath cells (Figure 3). However, fluorescence in Sh5 was only seen in a subset of the adult animals, suggesting lower endogenous *lim-7* expression (Figure 3). As expected, the URA neurons also expressed *lim-7*(+)*::mCherry*. Moreover, at least ten additional cells, which appear to be neuronal, expressed *lim-7*(+)*::mCherry* near the isthmus and terminal bulb of the pharynx in a similar region to the URA neurons (Figure 3). Late embryos also appear to express *lim-7*(+)*::mCherry* in the same region. The exact identity of these cells requires further confirmation as many different neurons reside in this region in addition to other cell types.

Since one prominent phenotype in *tm674* animals is Pun (Table 2), we looked closely for mCherry expression at the site of pharynx detachment. We did not observe mCherry expression at the detachment site within the pharynx or labia. A similar situation – the Pun phenotype without observable pharynx expression – has been observed for other genes (see Discussion).

The *lim-7*(+)*::mCherry* transgene was generated by recombineering, using one of the *lim-7*(+) fosmids we analyzed (WRM061aF09) and with which we observed partial rescue of the *lim-7*(*tm674*) phenotype. Unlike *lim-7*(+) transgenes, however, the *lim-7*(+)*::mCherry* transgene is integrated. We therefore tested it for rescue as well and found that it behaved identically to the *lim-7*(+) arrays described above, rescuing the lethality but not sterility of *tm674* (data not shown).

3.5 Intron 1 contains sequences necessary for expression in gonadal sheath cells

We are particularly interested in the control of *lim-7* expression in the somatic gonadal sheath. Therefore, we wanted to explore sequences contained in *tnIs5/6* that allow GFP expression in the gonadal sheath. In *C. elegans*, often a first intron longer than several hundred base pairs carries regulatory information [25] and the *lim-7* intron 1 is >1700 base pairs. Therefore, we explored whether gonadal sheath-specific regulatory elements might lie within intron 1. Hermaphrodites carrying intron 1 fused to GFP (pGC197) displayed GFP in all 10 pairs of gonadal sheath cells (Figure 1). The critical regulatory element within intron 1 was narrowed to a 45-bp region between base pairs 690 and 735 (Figure 1) that was both necessary and sufficient for expression of GFP in the gonadal sheath.

We queried the ALGGEN–PROMO database (http://alggen.lsi.upc.es) against all species and identified putative binding sites for 73 transcription factors in the intron 1 45-bp regulatory region, including sites for the *C. elegans* POU-homeodomain (POU-HD) transcription factor UNC-86. POU-HD transcription factors associate with LIM-HD proteins or regulate their expression (for examples see [26–28]). In *C. elegans*, one POU-HD protein, CEH-18, is expressed in the five pairs of gonadal sheath cells [29]. To test whether CEH-18 regulates *lim-7* expression in the gonadal sheath, we examined *lim-7*[*intron1::mCherry*] expression in two *ceh-18* null mutant backgrounds, *ceh-18*(*ok1082*) and the better-characterized *ceh-18*

(*mg57*). In both cases, the *lim-7*[*intron1::mCherry*] reporter was still expressed in the sheath (data not shown), suggesting that the intron 1 regulatory element is unresponsive to *ceh-18*. Thus, *ceh-18* does not appear to be an upstream regulator of *lim-7* expression in the gonadal sheath.

C. elegans is closely related to *C. remanei*, *C. brenneri* and *C. briggsae* and each contains a *lim-7* ortholog in a conserved genomic context, including a large first intron (ranging from 1746 bp in *C. brenneri* to 2452 bp in *C. remanei*). Alignment of the *C. elegans* 45-bp regulatory region with intron 1 from the three species did not reveal significant matches that provided clues regarding cis-acting factors. However, using the entire intron 1 of *C. elegans* as a query against intron 1 from the other species, we identified two conserved regions near the 3′ end of the intron 1. The first conserved region shares 21 nucleotides of identity among all four species (Figure 5 B). The second conserved region shares 22 nucleotides of identity in three of the four species (Figure 5 C). Thus, additional regulatory regions may exist within intron 1 that are dispensable for *lim-7* gonadal sheath expression, since intron 1 lacking those elements still retains expression in the sheath (Figure 1 A).

4. Discussion

4.1 *lim-7* is an essential gene

The *tm674* mutation of *lim-7* confers early larval lethality and phenotypic pleiotropy. The exon 4–5 deletion in *tm674* probably does not produce a functional protein product. Because many phenotypes are seen in L1 larvae, the LIM-7 transcription complex likely controls transcription of a diverse range of genes in late embryogenesis and the early L1 larval stage, and may involve more than one LIM-interacting factor to individuate regulation of these target genes.

4.2 The pleiotropic phenotypes of *lim-7*

The chief phenotype observed in *tm674* L1 larvae is Unc. Since *lim-7* is a member of the Islet family whose members are involved in motorneuron development, pathfinding and identity, it is not surprising that movement is affected. The *tm674* mutation perhaps could prevent proper formation or guidance of neurons to their correct position and result in an Unc phenotype.

Although LIM-7 expression is apparently absent within the pharynx, the *tm674* mutation results in an almost 50% penetrant Pun phenotype, detaching around the arcade cells. Similarly, *egl-18* (*elt-5*), results in a Pun phenotype (by RNAi) and its expression is not observed in the pharynx [30]. The labia of the worm connect to the buccal opening that then connects to the pharynx through specialized interfacial epithelial cells called arcade cells. Their primary function is to give continuity between the labia and the pharynx and flexibility to the connection between them when they undergo stress from foraging and pharyngeal pumping [31]. We speculate that this stress in the early L1 could cause separation of the two tissues. Alternatively, detachment may occur from failure of the URA motorneurons to form, to migrate, or direct processes to the correct location. URA motorneurons innervate head muscles and their cell bodies are positioned near the pharyngeal isthmus. Interestingly, their anteriorly-directed processes end approximately at the pharynx-buccal cavity junction [32], precisely where pharyngeal detachment occurs. Finally, the absence of *lim-7* expression in the pharynx could be due to limitations of the reporter (i.e., due to absence of required distant regulatory elements).

Approximately one-third of *tm674* L1 larvae have constipated intestines and another third are Dpy. The basis for these two phenotypes is unclear, but it is likely due to a requirement for LIM-7 in correct development or function of neuronal or intestinal tissues. The Dpy phenotype often results from a collagen defect. However, genes such as *dpy-22*, which encodes a mediator complex member, can display Dpy and/or Unc phenotypes when mutated [33,34]. Therefore,

Dpy defects in *lim-7*(*tm674*) may result from improper transcriptional control of a variety of genes. Additional more subtle phenotypes must exist since 5% of mutants appeared morphologically normal and yet all L1 mutant larvae die.

4.3 Partial rescue by *lim-7(+)*

Extrachromosomal arrays carrying *lim-7*(+) rescued L1 lethality caused by *lim-7*(*tm674*), but rescued worms were sterile or produced 1–2 L1 larvae that died. One possibility is that a sterility-inducing mutation is closely linked to the *lim-7* locus in the *tm674* strain. While we cannot completely rule out this possibility, the chromosome was outcrossed seven times, reducing the chances of a closely linked mutation. Another possibility is that *lim-7* activity is required in the germline. Since extrachromosomal arrays are usually silenced in the germline, our arrays would not compensate for required germline activity [35]. We note that sterility is consistent with roles already attributed to the somatic gonadal sheath (where *lim-7* is expressed), suggesting that improper levels of *lim-7*(+) somatic gonad expression could result in sterility [12,23]. At this time, we cannot distinguish between these possibilities. Therefore, barring the presence of a closely linked sterile mutation, our results suggest that *lim-7* may be important for fertility (Figure 4).

Using the 125-bp intron 1 regulatory element identified through gonadal sheath expression, only one to two neurons expressed GFP (Figure 1 D) while the full intron 1 drove expression in multiple head neurons (data not shown), suggesting that regulatory modules for individual or sets of neurons also reside within intron 1. Further isolation of specific enhancers within *lim-7* intron 1 may serve as useful cell-type specific markers.

4.4 A *lim-7* expression pattern

One aim of this study was to determine a more complete *lim-7* expression pattern. Our analysis reveals that reporter fusions containing different genomic sequences confer different expression patterns, suggesting that there is complex regulation of expression. The previous widely used *lim-7* reporter, *tnIs6*, contains sequences ~2.2 kb upstream and the first intron and first two exons of *lim-7* (altogether 4.1 kb). This construct shows expression in the URA motor neurons and in four of the five gonadal sheath pairs [11]. We examined the full-length *lim-7::mCherry* reporter, *stIs10289*, and found that it expressed in additional cells, both in the gonadal sheath and in the pharyngeal region (Figure 3). Another *lim-7* reporter, pUL#JRH8C3, bearing 1.5 kb upstream fused to GFP (with no *lim-7* intron sequences), confers yet a different expression pattern that includes previously observed embryonic expression but no gonadal sheath expression, as well as expression in a subset of muscle, intestinal and nerve cells in larval and adult stages [24]. We also created a reporter construct that contains only 2.2 kb upstream of *lim-7* fused to GFP and observed a similar but not identical expression pattern to that reported by Reece-Hoyes et al. [24]. For example, we did not see expression in the body wall muscle (data not shown).

Although all reporters we examined have overlapping and distinct expression patterns, *stIs10289* may best approximate the true *lim-7* expression pattern since the entire genomic context is included within the construct (>29 kb including 11.684 kb upstream, all introns and exons, and 9.309 kb downstream). In shorter constructs, omission of enhancer elements can either eliminate expression or cause spurious expression (e.g., by removal of a repressor binding sites that prevent expression in certain tissues).

4.5 *lim-7* intron 1 sequences are necessary and sufficient for expression in the gonadal sheath

We localized a gonadal sheath-specific enhancer to 45 bp within intron 1 between intron 1 base pairs 690 and 735, which is both necessary and sufficient for expression of GFP in the sheath

(PCR[690-735]; Figure 1 A). In addition, PCR[690-735] revealed that like the larger 125 bp element (pGC433 in Figures 1 A and 1 C) and the full-length *lim-7* reporter, GFP expression occurred in all five pairs of sheath cells per gonad arm. Expression of GFP in Sh5 was variable with *stIs10289*, pGC433, and PCR[690-735], which may reflect lower expression levels of *lim-7* within Sh5, close to the level of detection. Regardless, these constructs provide useful tools to further explore cis-acting elements regulating *lim-7* expression.

Acknowledgments

We thank the modEncode consortium for generously providing strain RW10289. We thank S. Mitani from the National Bioresource Project in Japan for providing *lim-7(tm674)*, and the Gene Knockout Project at OMRF and the *Caenorhabditis* Genetics Center for other strains. EJAH is supported by NIH GM061706.

Abbreviations

LIM-HD
: LIM-Homeodomain

POU-HD
: POU-Homeodomain

Sh1-5
: Gonadal Sheath Cell 1-5

References

1. Hobert O, Westphal H. Functions of LIM-homeobox genes. Trends Genet 2000;16:75–83. [PubMed: 10652534]
2. Dawid IB, Chitnis AB. LIM Homeobox Genes and the CNS: A Close Relationship. Neuron 2001;30:301–303. [PubMed: 11394990]
3. Klaus A, Saga Y, Taketo MM, Tzahor E, Birchmeier W. Distinct roles of Wnt/beta-catenin and Bmp signaling during early cardiogenesis. Proceedings of the National Academy of Sciences 2007;104:18531–18536.
4. Moretti A, Lam J, Evans S, Laugwitz K. Cardiovascular development: towards biomedical applicability. Cellular and Molecular Life Sciences (CMLS) 2007;64:674–682. [PubMed: 17380308]
5. Tao Y, Wang J, Tokusumi T, Gajewski K, Schulz RA. Requirement of the LIM Homeodomain Transcription Factor Tailup for Normal Heart and Hematopoietic Organ Formation in *Drosophila melanogaster*. Mol Cell Biol 2007;27:3962–3969. [PubMed: 17371844]
6. Weihe U, Milan M, Cohen SM. Regulation of Apterous activity in *Drosophila* wing development. Development 2001;128:4615–4622. [PubMed: 11714686]
7. Newman AP, Acton GZ, Hartwieg E, Horvitz HR, Sternberg PW. The *lin-11* LIM domain transcription factor is necessary for morphogenesis of *C. elegans* uterine cells. Development 1999;126:5319–26. [PubMed: 10556057]
8. Karlsson O, Thor S, Norberg T, Ohlsson H, Edlund T. Insulin gene enhancer binding protein Isl-1 is a member of a novel class of proteins containing both a homeo- and a Cys-His domain. Nature 1990;344:879–82. [PubMed: 1691825]
9. Wood WB. Determination of pattern and fate in early embryos of *Caenorhabditis elegans*. Dev Biol 1988;5:57–78.
10. Black B. Transcriptional pathways in second heart field development. Semin Cell Dev Biol 2007;18:67–76. [PubMed: 17276708]
11. Hall DH, Winfrey VP, Blaeuer G, Hoffman LH, Furuta T, Rose KL, Hobert O, Greenstein D. Ultrastructural features of the adult hermaphrodite gonad of *Caenorhabditis elegans*: relations between the germ line and soma. Dev Biol 1999;212:101–23. [PubMed: 10419689]

12. Killian DJ, Hubbard EJ. *Caenorhabditis elegans* germline patterning requires coordinated development of the somatic gonadal sheath and the germ line. Dev Biol 2005;279:322–35. [PubMed: 15733661]
13. Brenner S. The genetics of *Caenorhabditis elegans*. Genetics 1974;77:71–94. [PubMed: 4366476]
14. Shaner NC, Campbell RE, Steinbach PA, Giepmans BNG, Palmer AE, Tsien RY. Improved monomeric red, orange and yellow fluorescent proteins derived from Discosoma sp. red fluorescent protein. Nat Biotech 2004;22:1567–1572.
15. Mello C, Fire A. DNA transformation. Methods Cell Biology 1995;48:451–482.
16. Pepper AS, Killian DJ, Hubbard EJ. Genetic analysis of *Caenorhabditis elegans glp-1* mutants suggests receptor interaction or competition. Genetics 2003;163:115–32. [PubMed: 12586701]
17. Wood, W. The Nematode *Caenorhabditis elegans.* Cold Spring Harbor Press; Plainview, NY: 1988.
18. Edgley, MK.; Baillie, DL.; Riddle, DL.; Rose, AM. Genetic balancers. WormBook (The *C elegans* Research Community. 2006. WormBook (www.wormbook.org)
19. Rosenbluth RE, Baillie DL. The Genetic Analysis of a Reciprocal Translocation, *eT1*(III; V), in *Caenorhabditis elegans*. Genetics 1981;99:415–428. [PubMed: 6953041]
20. Wenick AS, Hobert O. Genomic cis-Regulatory Architecture and transActing Regulators of a Single Interneuron-Specific Gene Battery in *C. elegans*. Developmental Cell 2004;6:757–770. [PubMed: 15177025]
21. Etchberger JF, Hobert O. Vector-free DNA constructs improve transgene expression in *C. elegans*. Nat Methods 2008;5:3. [PubMed: 18165801]
22. Tatusova TA, Madden TL. BLAST 2 Sequences, a new tool for comparing protein and nucleotide sequences. FEMS Microbiol Lett 1999;174:247–250. [PubMed: 10339815]
23. McCarter J, Bartlett B, Dang T, Schedl T. Soma-germ cell interactions in *Caenorhabditis elegans*: multiple events of hermaphrodite germline development require the somatic sheath and spermathecal lineages. Dev Biol 1997;181:121–43. [PubMed: 9013925]
24. Reece-Hoyes JS, Shingles J, Dupuy D, Grove CA, Walhout AJ, Vidal M, Hope IA. Insight into transcription factor gene duplication from *Caenorhabditis elegans* Promoterome-driven expression patterns. BMC Genomics 2007;8:27. [PubMed: 17244357]
25. Okkema, PG.; Krause, M. Transcriptional regulation. WormBook (The *C elegans* Research Community. 2005. WormBook (www.wormbook.org)
26. Certel SJ, Thor S. Specification of *Drosophila* motoneuron identity by the combinatorial action of POU and LIM-HD factors. Development 2004;131:5429–39. [PubMed: 15469973]
27. Rockelein I, Rohrig S, Donhauser R, Eimer S, Baumeister R. Identification of amino acid residues in the *Caenorhabditis elegans* POU protein UNC-86 that mediate UNC-86-MEC-3-DNA ternary complex formation. Mol Cell Biol 2000;20:4806–13. [PubMed: 10848606]
28. Xue D, Finney M, Ruvkun G, Chalfie M. Regulation of the *mec-3* gene by the *C. elegans* homeoproteins UNC-86 and MEC-3. EMBO J 1992;11:4969–4979. [PubMed: 1361171]
29. Greenstein D, Hird S, Plasterk RH, Andachi Y, Kohara Y, Wang B, Finney M, Ruvkun G. Targeted mutations in the *Caenorhabditis elegans* POU homeo box gene *ceh-18* cause defects in oocyte cell cycle arrest, gonad migration, and epidermal differentiation. Genes Dev 1994;8:1935–48. [PubMed: 7958868]
30. Koh K, Rothman JH. ELT-5 and ELT-6 are required continuously to regulate epidermal seam cell differentiation and cell fusion in *C. elegans*. Development 2001;128:2867–2880. [PubMed: 11532911]
31. Mango, SE. The *C. elegans* pharynx: a model for organogenesis. WormBook (The *C elegans* Research Community. 2007. WormBook (www.wormbook.org)
32. White JG, Southgate E, Thomson JN, Brenner S. The structure of the nervous system of the nematode *Caenorhabditis elegans.* Phil Trans Royal Soc London, Series B Biol Scien 1986;314:1–340.
33. Yoda A, Kouike H, Okano H, Sawa H. Components of the transcriptional Mediator complex are required for asymmetric cell division in *C. elegans*. Development 2005;132:1885–1893. [PubMed: 15790964]
34. Simmer F, et al. Genome-Wide RNAi of *C. elegans* Using the Hypersensitive *rrf-3* Strain Reveals Novel Gene Functions. PLoS Biology 2003;1:e12. [PubMed: 14551910]

35. Kelly WG, Xu S, Montgomery MK, Fire A. Distinct requirements for somatic and germline expression of a generally expressed *Caenorhabditis elegans* gene. Genetics 1997;146:227–38. [PubMed: 9136012]

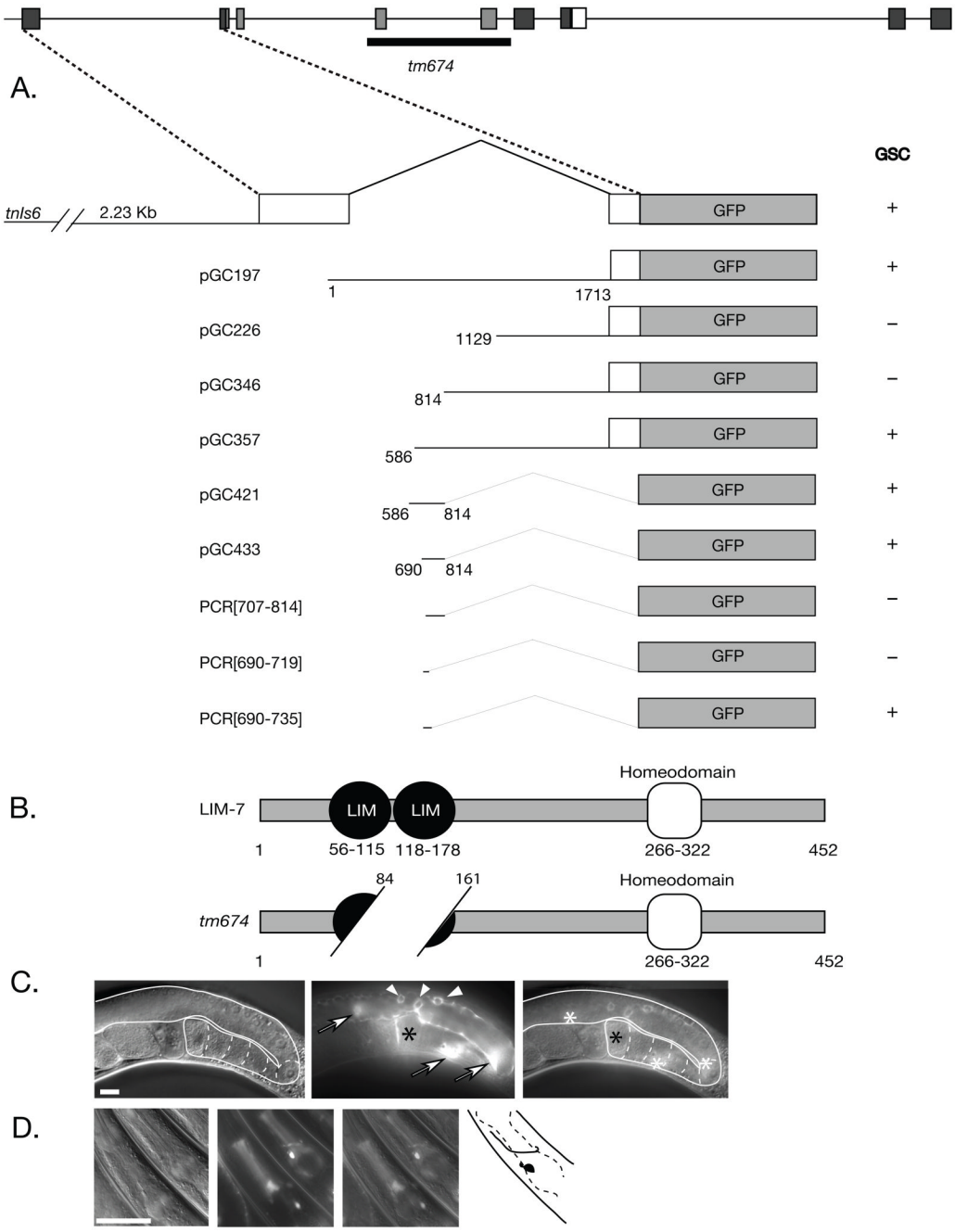

Figure 1. The *lim-7* locus and reporter constructs, LIM-7 structure, and gonadal sheath expression of the Intron 1 element

(A) Upper, *lim-7* genomic structure. Black and white exons correspond to domains of LIM-homeodomain proteins depicted in (B): black, LIM-domains; and white, homeodomain; dark gray, non-domain sequences. Lower, intron 1 fusions to GFP. (+), expression in the gonadal sheath; (−), no expression in the gonadal sheath; numbering refers to nucleotides from the beginning of intron 1. (B) LIM-7 LIM-HD protein structure and predicted *tm674* mutant protein structure. Color scheme as in (A). (C) Expression of pGC433 in the gonadal sheath. Gonad is outlined and maturing oocytes are outlined by dashed lines. Arrows indicate the nuclei of the thin gonadal sheath cells in plane of focus; arrowheads indicate germ cell nuclei surrounded

by gonadal sheath (fluorescence comes from sheath); black asterisk marks the proximal end of the gonad, where sheath pair 5 is located (fluorescence to left of asterisk may be due to *lim-7* (+)*::mCherry* fluorescence in Sh5; white asterisks in merge depicts the location of the three sheath nuclei in focus. (D) Expression of pGC433 in the head. Note neuron with anteriorly directed process encircling pharyngeal isthmus in upper animal (depicted in black in cartoon to right of images). (C) and (D): Left panel, DIC; middle panel, GFP fluorescence; right panel, merged image. Scale bar, 20 μm.

Figure 2. Terminal phenotypes of *tm674*.

Major phenotypes of *lim-7*(*tm674*) include Unc, Pun, Dpy, constipation, defective head morphology, and increased body vacuolarization. All images are of L1 larvae visualized using DIC optics. (A) Unc, Pun and constipation phenotypes. (B) Head bump, normal pharyngeal attachment, and increased body vacuoles. (C) Dpy, Pun and constipation. (D) Rare gross head malformation. Inset is magnification of head for better detail. Arrowheads in A, B, C, end of pharynx; Arrows in A, C, distended intestine; * in B, body vacuoles. Scale bars, 20 μm.

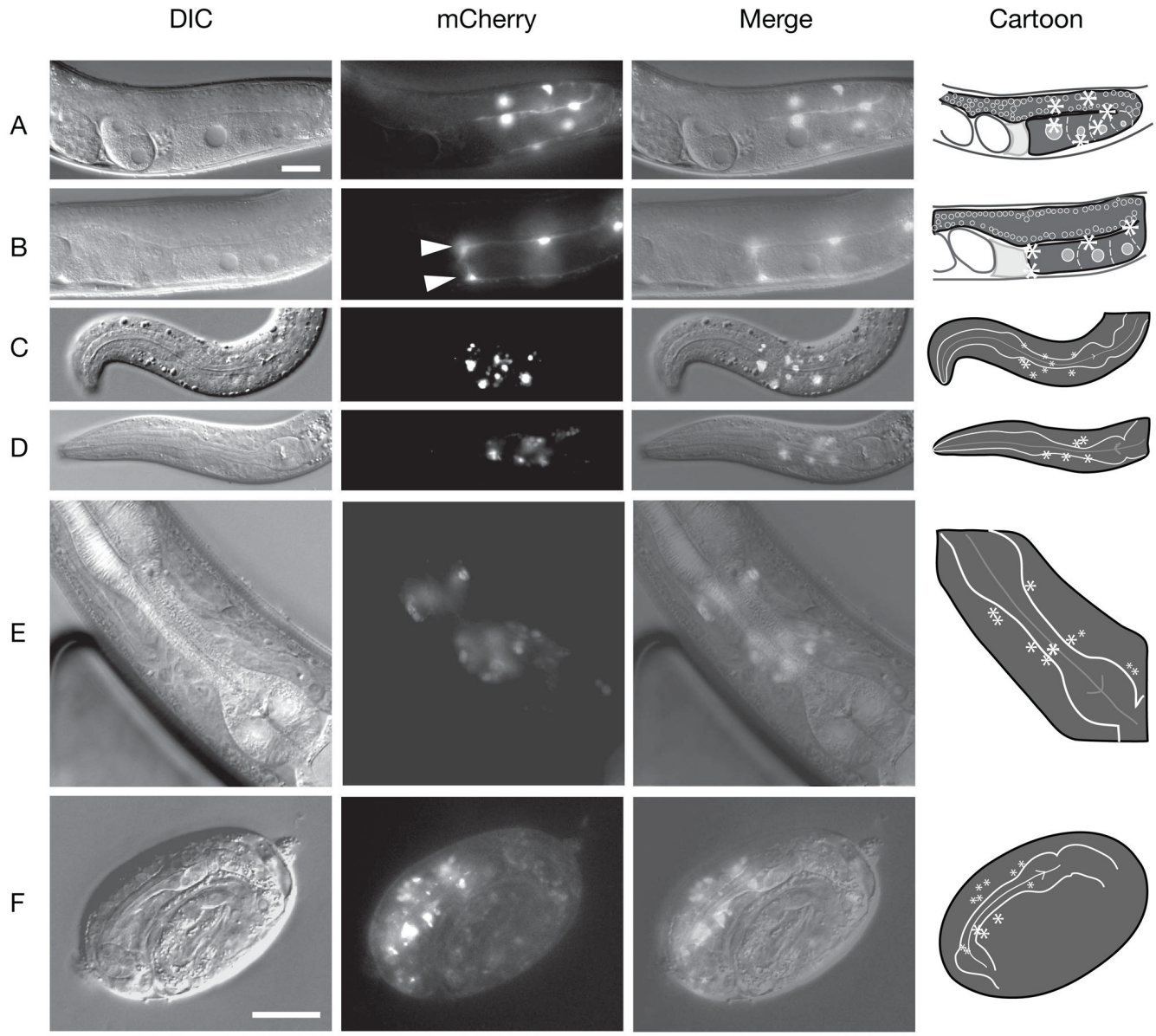

Figure 3. Expression pattern of a *lim-7*(+)*::mCherry* fosmid-based reporter

RW10289 animals were examined for mCherry fluorescence. Because the gonadal sheath is a very thin tissue that surrounds the proximal two-thirds of the gonad, sheath nuclei are difficult to discern without a fluorescent marker. (A) Adult gonad showing six sheath cell nuclei; additional expressing sheath nuclei out of focal plane. (B) Adult gonad showing sheath pair five expressing *lim-7*(+)*::mCherry* plus two other sheath nuclei. Arrowheads mark sheath pair five nuclei. In A and B cartoons, sheath nuclei depicted by white asterisks; pale gray structure, spermatheca; large white ovals, fertilized embryos; maturing oocytes outlined by dashed lines. (C) and (D) L1 larvae expressing *lim-7*(+)*::mCherry* in URA neurons and additional cells near the pharyngeal isthmus. (E) Adult pharyngeal expression. (F) Late embryo pharyngeal isthmus expression. Drawing includes only pharyngeal bulbs and isthmus of the embryo; other regions of embryo not drawn. (C–F) Asterisks in drawings represent main fluorescent nuclei location in pharyngeal region. Left, DIC; middle, *lim-7*(+)*::mCherry* expression; right, merged image;

far right, cartoon of relevant structures in each panel. (C – F), asterisks represent fluorescent nuclei. Scale bars, 20 μm.

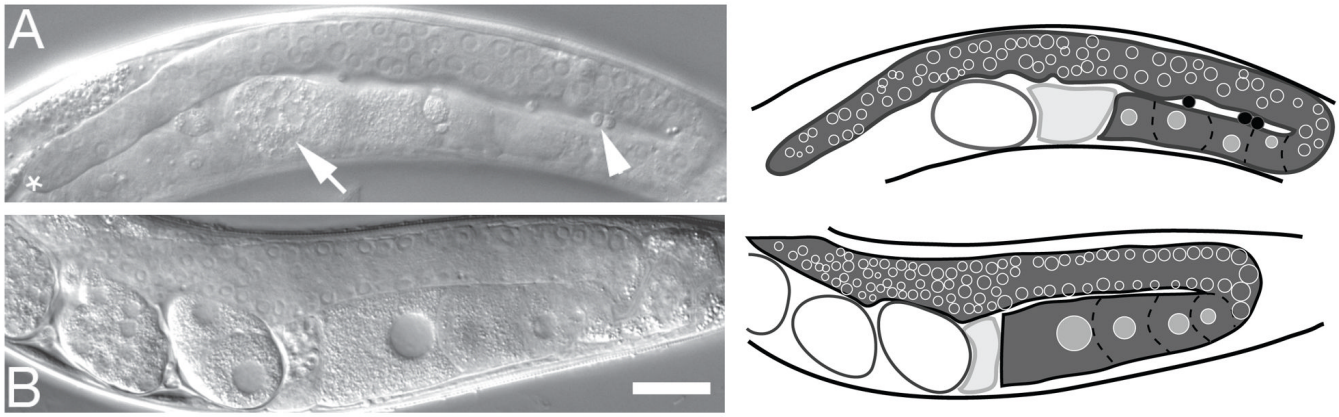

Figure 4. *tm674* hermaphrodites bearing a *lim-7*(+) transgene exhibit gonadal defects resulting in sterility

(A) Adult gonad from *tm674; lvEx4*[*lim-7*(+); *sur-5::GFP*] (strain HN15, see Materials and Methods section 2.1). Distal gonad marked by (*), single disintegrating embryo in the uterus (white arrow), and loose sperm, (white arrowhead). (B) RW10289 gonad for comparison. Cartoon of each gonad (in dark gray) is to the right: Maturing oocytes outlined by dashed lines and immature germ cell nuclei indicated by open circles. The proximal gonad is adjacent to the spermatheca, in pale gray; embryos are open ovals to the left of spermatheca; black filled circles in (A) are loose sperm. Scale bar, 20 μm.

A.

```
690  TTTAAAAGAAAACAAAAATCGCTATTTCTTTCATTCCATTTGTCCCCCTCCTCTTTTACTTTT
     TTCTTTTCCACCTTCTTCTTGTTGTCTTAAAAACGCATAACTTCATCTGGTCCTTCGATGAA  814
```

B.

```
C. elegans      1454  AACACCCCACAAATGAGCTATTTTATGAGTTTTGTTAGGCTCT  1496
                      ||  |  | ||||||||||||||||||||||  |    |   | |
C. briggsae     1475  AACACTCGACAAATGAGCTATTTTATGAGCTTTGTTAGGCTCT  1517
                      ||  |  | ||||||||||||||||||||||  |    |   | |
C. remanei      2248  CACCCTCCACAAATGAGCTATTTTATGAGGGTCCGCACTTTTT  2290
                      ||  |  | ||||||||||||||||||||||  |    |   | |
C. brenneri     1450  AACACCCCACAAATGAGCTATTTTATGAGCTTTGTTAGGCTTT  1492
```

C.

```
C. elegans      1623 CTCCCCTCCTCTCACAAACCCTGTAATCTTCAAATCAAAGTCGA  1666
                     |||    |  ||       ||||||||||||||||||||
C. briggsae     1658 CTCTATTTCT GAGCAAACCCTGTAATCTTCAAATCAACCCTTC  1702
                     |||    |  ||       ||||||||||||||||||||
C. remanei      2334 CTCCCCTCCTCAACTTAACCCTGTAATCTTCAAATCAACCGATT  2377
```

Figure 5. Intron 1 sequence elements from *lim-7* orthologs in four *Caenorhabditis* species

(A) The 125-bp region in intron 1 necessary for gonadal sheath expression; bold underlined nucleotides (690 – 735) are necessary and sufficient for expression in the gonadal sheath. (B) The highlighted 21-nt element conserved in all four species. (C) The highlighted 22-nt element conserved in three of the four species. All numbering begins from first nucleotide of the 5′ end of intron 1.

Table 1

lim-7(tm674) mutants display L1 larval lethality

Genotype	% L1 larvae[1] (n)[2]
tm674	17.9 (165)
tm674/hT2 [let GFP]	82.1 (757)

[1] Percentage of total larvae counted over two-hour intervals

[2] n = Total number of larvae counted

Table 2

Penetrance of phenotypes seen in *lim-7(tm674)* L1 larvae

Phenotypes[1]	**Penetrance in % (n) for *tm674*[2]**
Unc[3]	74% (140)
Pun[4]	43% (141)
Constipation[5]	36% (136)
Dpy[6]	34% (141)
Body cavities[7]	23% (142)
Abnormal head morphology[8]	12% (139)

[1] Major phenotypes observed for *lim-7(tm674)* during L1 stage prior to death. Other rare phenotypes are not presented in this table (e.g. see Figure 2 D).

[2] Penetrance of *tm674* L1 larvae exhibiting defect. (n) = total number of animals evaluated.

[3] Abnormal body position indicative of an Unc animal. (Figure 2).

[4] Pharynx unattached (Figures 2 A and C).

[5] Abnormal distension of the intestinal lumen (Figures 2 A and C).

[6] Increased overall body width compared to length (Figure 2 C).

[7] Increased appearance of body vacuoles (Figure 2 B).

[8] Includes one or more head bumps (Figure 2 B).